

# Gradient-based Algorithms for Machine Teaching

## Supplementary Materials

Pei Wang  
UC, San Diego  
pew062@ucsd.edu

Kabir Nagrecha  
UC, San Diego  
kabir.nagrecha@gmail.com

Nuno Vasconcelos  
UC, San Diego  
nuno@ucsd.edu

### A. Appendix

#### A.1. Proof of Corollary 1

**Proof** Under the optimal student assumption, the predictor learned by the student at iteration  $t$  is

$$f^t = \arg \min_f \mathcal{R}_{\mathcal{L}^t}[f] = \arg \min_f \sum_{(x_i, y_i) \in \mathcal{L}^t} \phi(y_i f(x_i)). \quad (30)$$

If the teacher selects at least one new example per iteration,  $\mathcal{L}^t$  increases with  $t$ , i.e.  $\mathcal{L}^{t-1} \subset \mathcal{L}^t$ . Since  $\mathcal{D}$  has finite size  $n$ ,  $\exists k \leq n$  s.t.  $\mathcal{L}^k = \mathcal{D}$ . It follows that, if  $\zeta \geq |\mathcal{D}|$ , the student will eventually learn from  $\mathcal{L}^k$ . From (30) and (1) it follows that  $f^k = f^*$ . ■

#### A.2. Proof of Lemma 1

**Proof** Assume without loss of generality that  $\mathcal{A} = \{(x_1, y_1), \dots, (x_m, y_m)\}$  and  $\mathcal{B} = \{(x_{m+1}, y_{m+1}), \dots, (x_n, y_n)\}$  for any  $1 < m < n$ . Then, it follows from (10) that

$$\nabla_{\Psi(\mathcal{D})}^T R_{\mathcal{D}}(f) = (w_1, \dots, w_m, w_{m+1}, \dots, w_n)^T \quad (31)$$

$$= \left( \nabla_{\Psi(\mathcal{A})}^T R_{\mathcal{A}}(f), \nabla_{\Psi(\mathcal{B})}^T R_{\mathcal{B}}(f) \right) \quad (32)$$

$$= \left( \nabla_{\Psi(\mathcal{A})}^T R_{\mathcal{A}}(f), 0 \right) + \left( 0, \nabla_{\Psi(\mathcal{B})}^T R_{\mathcal{B}}(f) \right) \quad (33)$$

$$= \nabla_{\Psi(\mathcal{D})}^T R_{\mathcal{A}}(f) + \nabla_{\Psi(\mathcal{D})}^T R_{\mathcal{B}}(f) \quad (34)$$

and (18) follows from (8). ■

#### A.3. Proof of Lemma 2

**Proof** Assume, without loss of generality, that  $\mathcal{L}^{t-1}$  contains examples  $\{x_i\}_{i=1}^k$  and  $\mathcal{D}^{t-1}$  examples  $\{x_i\}_{i=k+1}^n$ , for some  $1 < k < n$ . Then

$$\nabla_{\Psi(\mathcal{D})}^T R_{\mathcal{L}^{t-1}}(f^t) = \left( \nabla_{\Psi(\mathcal{L}^{t-1})}^T R_{\mathcal{L}^{t-1}}(f^t), \nabla_{\Psi(\mathcal{D}^{t-1})}^T R_{\mathcal{L}^{t-1}}(f^t) \right) \quad (35)$$

$$= \left( \nabla_{\Psi(\mathcal{L}^{t-1})}^T R_{\mathcal{L}^{t-1}}(f^t), 0 \right). \quad (36)$$

Since the student is optimal, (30) holds and, using (13),  $\nabla_{\Psi(\mathcal{L}^{t-1})} R_{\mathcal{L}^{t-1}}(f^t) = 0$ . Hence,  $\nabla_{\Psi(\mathcal{D})} R_{\mathcal{L}^{t-1}}(f^t) = 0$  and, from (8),  $\partial_g R_{\mathcal{L}^{t-1}}(f^t) = 0$ . Since, from Lemma 1,

$$\partial_g R_{\mathcal{D}}(f^t) = \partial_g R_{\mathcal{L}^{t-1}}(f^t) + \partial_g R_{\mathcal{D}^{t-1}}(f^t), \quad (37)$$

(19) follows. ■

#### A.4. Proof of Theorem 1

**Proof** For any  $g = \sum_{x_i \in \mathcal{D}} \alpha_i \delta(x - x_i)$ ,  $\|g\| = 1$  if and only if  $\|\alpha\| = 1$  and, from (8),

$$\begin{aligned} \partial_g R_{\mathcal{D}}(f^t) &= \langle \nabla_{\Psi(\mathcal{D})} R_{\mathcal{D}}(f^t), \alpha \rangle \geq \\ &= -\|\nabla_{\Psi(\mathcal{D})} R_{\mathcal{D}}(f^t)\| \|\alpha\| = -\|\nabla_{\Psi(\mathcal{D})} R_{\mathcal{D}}(f^t)\|. \end{aligned} \quad (38)$$

Since equality is achieved when  $\alpha$  is the direction

$$\alpha^* = -\frac{1}{\|\nabla_{\Psi(\mathcal{D})} R_{\mathcal{D}}(f^t)\|} \nabla_{\Psi(\mathcal{D})} R_{\mathcal{D}}(f^t), \quad (39)$$

the steepest descent solution of (15) is

$$g^* = \sum_{x_i \in \mathcal{D}} \alpha_i^* \delta(x - x_i) \quad (40)$$

Similarly, the steepest descent direction of (17) is

$$h^*(\mathcal{L}) = \sum_{x_i \in \mathcal{L}} \nu_i^* \delta(x - x_i) \quad (41)$$

with

$$\nu^* = -\frac{1}{\|\nabla_{\Psi(\mathcal{L})} R_{\mathcal{L}}(f^t)\|} \nabla_{\Psi(\mathcal{L})} R_{\mathcal{L}}(f^t), \quad (42)$$

Assuming, without loss of generality, that  $\exists k$  such that  $x_i \in \mathcal{L}$  for  $i < k$ , then

$$h^*(\mathcal{L}) = \sum_{x_i \in \mathcal{D}} \beta_i^* \delta(x - x_i) \quad (43)$$

where

$$(\beta^*)^T = (\nu^T, 0) = -\frac{1}{\|\nabla_{\Psi(\mathcal{D})}R_{\mathcal{L}}(f^t)\|} \nabla_{\Psi(\mathcal{D})}^T R_{\mathcal{L}}(f^t), \quad (44)$$

and

$$\langle g^*, h^*(\mathcal{L}) \rangle = \langle \alpha^*, \beta^* \rangle \quad (45)$$

$$= \left\langle -\frac{1}{\|\nabla_{\Psi(\mathcal{D})}R_{\mathcal{D}}(f^t)\|} \nabla_{\Psi(\mathcal{D})} R_{\mathcal{D}}(f^t), \right. \\ \left. -\frac{1}{\|\nabla_{\Psi(\mathcal{D})}R_{\mathcal{L}}(f^t)\|} \nabla_{\Psi(\mathcal{D})} R_{\mathcal{L}}(f^t) \right\rangle \quad (46)$$

$$= \frac{\|\nabla_{\Psi(\mathcal{D})}R_{\mathcal{L}}(f^t)\|^2}{\|\nabla_{\Psi(\mathcal{D})}R_{\mathcal{D}}(f^t)\| \|\nabla_{\Psi(\mathcal{D})}R_{\mathcal{L}}(f^t)\|} \quad (47)$$

$$= \frac{\|\nabla_{\Psi(\mathcal{D})}R_{\mathcal{L}}(f^t)\|}{\|\nabla_{\Psi(\mathcal{D})}R_{\mathcal{D}}(f^t)\|}, \quad (48)$$

where we have used the fact that

$$\nabla_{\Psi(\mathcal{D})}^T R_{\mathcal{D}}(f^t) = \left( \nabla_{\Psi(\mathcal{D})}^T R_{\mathcal{L}}(f^t), \nabla_{\Psi(\mathcal{D})}^T R_{\mathcal{D}-\mathcal{L}}(f^t) \right). \quad (49)$$

It follows that the solution of (16) is

$$\mathcal{N}^t = \arg \max_{\mathcal{N} \in \mathcal{P}^t} \|\nabla_{\Psi(\mathcal{D})} R_{\mathcal{L}^{t-1} \cup \mathcal{N}}(f^t)\|^2. \quad (50)$$

$$= \arg \max_{\mathcal{N} \in \mathcal{P}^t} \{ \|\nabla_{\Psi(\mathcal{D})} R_{\mathcal{L}^{t-1}}(f^t)\|^2 + \|\nabla_{\Psi(\mathcal{D})} R_{\mathcal{N}}(f^t)\|^2 \} \quad (51)$$

$$= \arg \max_{\mathcal{N} \in \mathcal{P}^t} \|\nabla_{\Psi(\mathcal{D})} R_{\mathcal{N}}(f^t)\|^2 \quad (52)$$

$$= \arg \max_{\mathcal{N} \in \mathcal{P}^t} \|\nabla_{\Psi(\mathcal{N})} R_{\mathcal{N}}(f^t)\|^2 \quad (53)$$

where we have used the fact that, from Lemma 2,  $\|\nabla_{\Psi(\mathcal{D})} R_{\mathcal{L}^{t-1}}(f^t)\|^2 = 0$ . ■

## B. Other implementation details

Both datasets were subject to standard normalizations. Training images were first randomly resized to  $224 \times 224$  and then randomly flipped, whereas testing images were first resized to  $256 \times 256$  and then center-cropped to  $224 \times 224$ . All images were also first converted to  $[0.0, 1.0]$  from  $[0, 255]$  and then normalized by subtracting the mean  $[0.485, 0.456, 0.406]$  and dividing by the standard deviation  $[0.229, 0.224, 0.225]$  of each RGB color channel. On both datasets, we use the train-test split of [2]. The data is accessible in [1]. The 512-D output of global average pooling of the ResNet-18 is used for the output of  $f(x)$  on the multiclass case. More details are available in our attached code. In real learner evaluation, we require that workers be masters to do our tasks. Additionally, we require non-Chinese speaker on Chinese Characters dataset experiments. Each turker is paid \$1 for the teaching task.

## C. Selected teaching examples

We show the selected teaching images of MaxGrad on both datasets in Figure 1 and 2. Also, Figure 3 shows histograms of test time accuracy, at the end of the training. MaxGrad is clearly more effective than RANDOM overall.

## References

- [1] Oisín Mac Aodha, Shihan Su, Yuxin Chen, Pietro Perona, and Yisong Yue. [https://github.com/macodha/explain\\_teach/tree/master/data](https://github.com/macodha/explain_teach/tree/master/data).
- [2] Oisín Mac Aodha, Shihan Su, Yuxin Chen, Pietro Perona, and Yisong Yue. Teaching categories to human learners with visual explanations. In *Proceedings of the IEEE Conference on Computer Vision and Pattern Recognition*, pages 3820–3828, 2018.

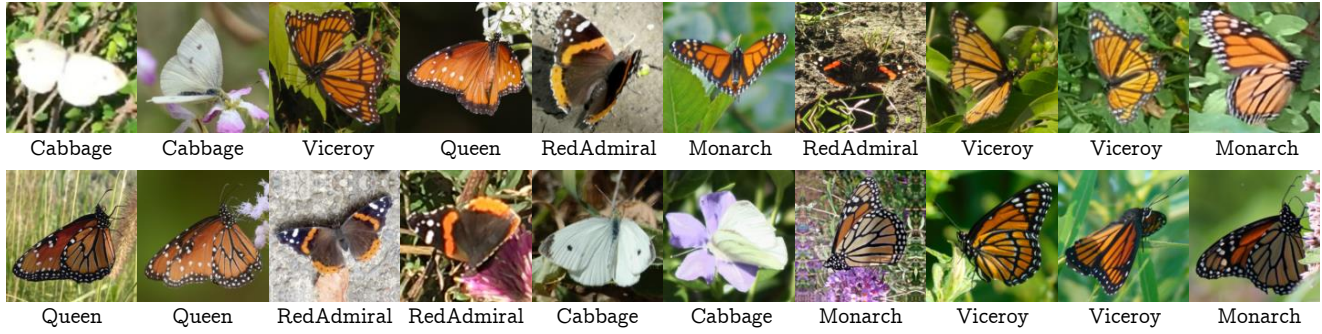


Figure 1: Selected teaching images on Butterflies

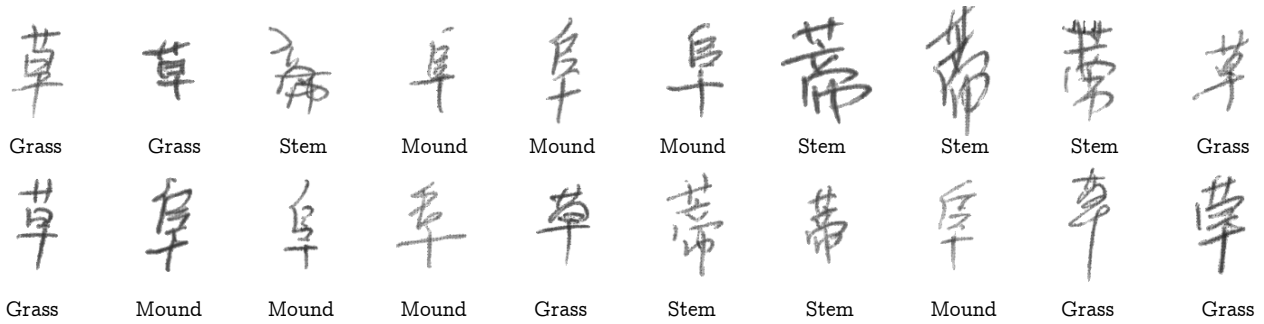


Figure 2: Selected teaching images on Chinese Characters

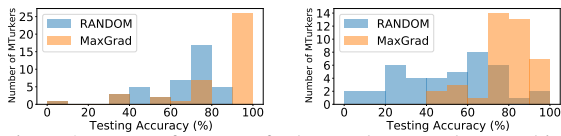


Figure 3: Test performance for human learners: learners binned by test accuracy. Left: Butterflies. Right: Chines chars.